Quasi-Phase Matched Second-Harmonic Generation in Telluride Compounds Using Total Internal Reflection

Sumita Deb
Electrical Engineering Department, NIT, Agartala
Barjala, Jirania, Tripura, India

Ardhendu Saha
Electrical Engineering Department, NIT, Agartala
Barjala, Jirania, Tripura, India

Smita Banik
Electrical Engineering Department, NIT, Agartala
Barjala, Jirania, Tripura, India

Upama Das
Electrical Engineering Department, NIT, Agartala
Barjala, Jirania, Tripura, India

***Abstract*—We analytically describe quasi-phase matched second-harmonic generation in the mid-IR region in a parallel isotropic semiconductor slab made of Zinc Telluride (ZnTe) and Cadmium Telluride (CdTe) using total internal reflection quasi phase matching technique. The simulated results indicate conversion efficiencies of 4.08% (centered at 8.495 µm) and 15.83% (centered at 9.341 µm) in a 400 µm thick, 10-mm-long slab of ZnTe and CdTe respectively. The losses due to surface roughness, Goos-Hänchen shift and absorption of the slab have been considered in the analysis. The effect of variation in the angle of incidence has been studied for both the materials.**

Keywords-second-harmonic generation, total internal reflection, quasi phase matching, isotropic, zinc telluride, cadmium telluride.

I. INTRODUCTION

Mid-infrared tunable sources are of considerable interest for applications in environmental monitoring. Indeed, the main civilian and military pollutants present strong absorbing lines in the spectral region from 3 to 12 µm [1]. In this context, quasi-phase matching (QPM) has proven to be the most promising technique in the generation of tunable optical sources because of its ability to phase-match any two waves by choosing an appropriate spatial period of modulation of the nonlinear coefficient along the propagation direction within the transparency region of the chosen material.

Rapid development in the field of semiconductor technology has lead to extensive use of isotropic semiconductors for optical frequency conversion techniques. These isotropic semiconductors offer a number of advantages like (i) high optical second-order nonlinear susceptibility, (ii) excellent transparency range, (iii) good mechanical properties, (iv) possible future integration with the pumping source etc. [2]. Among these semiconductors, ZnTe and CdTe have indeed come forward as an important nonlinear optical crystals, finding wide applications in generation of pulsed terahertz radiation in time-domain terahertz spectroscopy, terahertz imaging, holographic interferometry, optical rectification, reconfigurable optical interconnections, infrared optical window, photovoltaics and in laser optical phase conjugation devices [3]. However, these compounds being isotropic, no natural birefringence phase matching is possible. Therefore, QPM may be considered an attractive technique for frequency generation in these isotropic crystals.

It was 1962 when Armstrong *et al.* first suggested that QPM can be obtained by total internal reflection (TIR) in a plane parallel slab [4]. This technique has been demonstrated in isotropic semiconductor (GaAs, ZnSe, ZnS) slabs for resonant-QPM as well as nonresonant QPM by a number of researchers [5-7]. Both resonant as well as nonresonant QPM techniques make use of differential Fresnel phase shift $\Delta\phi_F$ experienced by the three interacting waves at reflection at the air-material interface. This phase shift $\Delta\phi_F$ can compensate for the dispersion phase mismatch $\Delta k = k_3 - 2k_1$ (here k_1 and k_3 represents the fundamental and SH wave vectors respectively) and allows a quasi-phase matched growth of the conversion signal. The basic difference between resonant and nonresonant QPMs lies in the bounce length between two consecutive TIR bounces. In case of resonant QPM, the bounce length is exactly equal to an odd multiple of the coherence length whereas nonresonant refers to the situation where the bounce length is not exactly equal to an odd multiple but also not equal to an even multiple as well. Thus the phase matching

Proc. of the International Conference on Pervasive Computing and Communication (PCC)
Editor In Chief Dr. R. K. Singh.

ISBN: 978-981-07-2579-2

conditions are more stringent in resonant as compared to nonresonant scenario.

II. PROPOSED SCHEME

We have considered a parallel semiconductor slab (Fig. 1) of length, L = 10 mm, and thickness, t = 400 μm. The face on which the fundamental laser radiation will be incident is cut at an angle ψ (= 0.39 rad) with respect to a plane perpendicular to the horizontal plane.

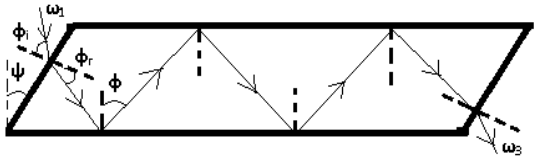

Figure 1. Geometry of parallel semiconductor slab showing the scheme of second harmonic frequency conversion.

Let the fundamental broadband optical radiation having centre frequency ω_1 be incident at an angle φ_i with respect to the normal to the inclined slab end face. The angle of incidence φ_1 on the horizontal plane inside the semiconductor slab will be determined by the refractive index of the material. If φ_1 is greater than the critical angle for the range of input frequencies, then the collimated optical radiation will undergo TIR inside the tapered slab. This scheme corresponds to non-resonant QPM since the interaction lengths between successive bounces has not been optimized to be equal to an odd multiple of the coherence length L_{coh} (=π/Δk).

Now, in this parallel slab configuration with simple geometry the equation for the length between consecutive bounces can be expressed in terms of slab parameters as follows:

$$L_1 = x\cos\psi/[\sin(\varphi_r+\psi)] \quad (1)$$

where L_1 is the length between the entrance point and the point of first TIR point inside the slab, x is the slant distance of the entrance point from the base of the slab, and

$$\varphi_r = \sin^{-1}[(\sin\varphi_i)/n_1] \quad (2)$$

where n_1 is the refractive index corresponding to the input fundamental frequency. The distance between successive bounces can be expressed as

$$L_i = t/\cos\varphi \quad (3)$$

where $\varphi = \pi/2 - (\varphi_r + \psi)$ is the angle of incidence inside the slab.

A. Polarization Configuration

In general there are eight possible polarization combinations of the three interacting waves ($\omega_1, \omega_2, \omega_3$) ($\omega_1, \omega_2$ are input wavelengths, ω_3 is the generated output wavelength):

1. *sss* and *ppp* (Type 0 phase matching)
2. *ssp* and *pps* (Type I phase matching)
3. *psp, spp, pss, sps* (Type II phase matching)

The designations refer to the orientation of the electric field vector in each wave relative to the plane of incidence, wherein '*s*' designates the polarization that is orthogonal to the plane of incidence and '*p*' denotes the orientation of electric field parallel to the plane of incidence.

In our analysis we have considered *ppp* polarization configuration for both ZnTe and CdTe crystals. According to Komine *et al.*, ppp is the most useful polarization configuration, in which the net phase shift quickly approaches π over a wide range of incidence angles [6].

The expression for effective d-coefficient for *ppp* polarization can be expressed as follows:

$$d_{ppp} = 6d_{ij}\cos^2\varphi\sin\varphi\cos\tau\sin\tau \quad (4)$$

with the slab orientation in the {001} direction, where τ is the angle that the plane of incidence makes with the {100} direction. The d-coefficient is maximum for τ = 45° [6]. Since ZnTe and CdTe have the same zinc blended crystallographic structure, their non-linear coefficient can be expressed by the same function. Here d_{ij} is d_{14} since both ZnTe and CdTe belong to symmetry class $\bar{4}3m$. The value of d_{14} is considered to be 90 pm/V for ZnTe and 168 pm/V for CdTe [8].

B. Sellemier's Equation

The standard Sellemier's equation can be expressed as $n^2 = A + [B\lambda^2/(\lambda^2 - c^2)]$ where n is the refractive index and λ is the wavelength in microns. For ZnTe the best values of the parameters are A=4.27, B=3.01, and c^2=0.142; and for CdTe, A=5.68, B=1.53, and c^2=0.366 [9].

C. Conversion Yield Limiting Factors

The SHG conversion efficiency is limited by three important factors: the surface roughness, the Goos-Hänchen shift, and the absorption loss of the material. All these factors are considered in our analysis.

The drop due to residual surface roughness is measured in terms of the Strehl ratio [7], which gives the reflection coefficient, R as a function of wavelength, angle of incidence, and standard deviation,

$$R = \exp[-\{(4\pi n_j\sigma\cos\varphi_n)/\lambda_j\}^2] \approx 1 - \{(4\pi n_j\sigma\cos k\varphi_n)/\lambda_j\}^2 \quad (5)$$

where j = ω for the fundamental wave and 2ω for the generated SH, and σ(= p−v value/12) where the p−v value is the distance between the peak and valley of the surface

under consideration. A p−v value of 150 nm is considered in the computer-aided simulation.

When a collimated light beam is totally reflected from a plane interface between two dielectric media, the reflected beam encounters a longitudinal shift between the incident and reflected beams known as the Goos-Hänchen (GH) shift) [10]. This longitudinal shift causes a reduction of the usable length of the semiconductor slab. In our case, the GH shift has been separately calculated for the lower horizontal surface and the inclined upper surface.

Linear absorption can be highly detrimental to frequency conversion processes and places severe limits on conversion efficiency values. In our analysis we consider a linear absorption coefficient ($\alpha_\omega \approx \alpha_{2\omega}$) of 0.008 cm^{-1} for ZnTe and 0.0014 cm^{-1} for CdTe [8].

D. SH Intensity

The generated SH intensity in the undepleted plane wave approximation is given by:

$$I_3^{out} = [z_0\omega_3^2(Nd_{eff})^2/(2c^2n_1n_2n_3)]*[\sin(\Delta kL/2)/(\Delta k/2)]^2*[\sin(N\Delta\phi/2)/(N\sin(\Delta\phi/2))]^2*I_1^{in}*I_2^{in} \quad (6)$$

Where, $I_1^{in} = I_2^{in}$ is the input fundamental intensity, N is the number of bounces inside the plate, z_0 is the vacuum impedance (= 377 Ω).
The global phase shift $\Delta\phi = \Delta kL + \Delta\phi_F + \delta\phi$ where L is the distance between two successive bounces (given by equ^n 3).

In our analysis the interaction length between the last bounce and the exit point from the semiconductor slab is not considered. The effects of linear absorption and surface roughness on both the fundamental and the generated SH waves are included for all the consecutive bounces inside the slab. The reduction in the usable length of the semiconductor slab due to the GH shift is also considered in the analysis.

III. Results and Discussions

In the computer-aided simulation, the input beam intensity is assumed to be $I_\omega \approx 10$ MW/cm^2. The analysis uses an input fundamental broadband source of 8−10 μm. The input conditions at the entry point of the collimated optical beam to the semiconductor slab are chosen as ϕ_i = 1.4 rad and x = 50 μm. The variation of SH efficiency with respect to the input fundamental wavelength is shown in Fig.2 and Fig. 3 for ZnTe and CdTe respectively.

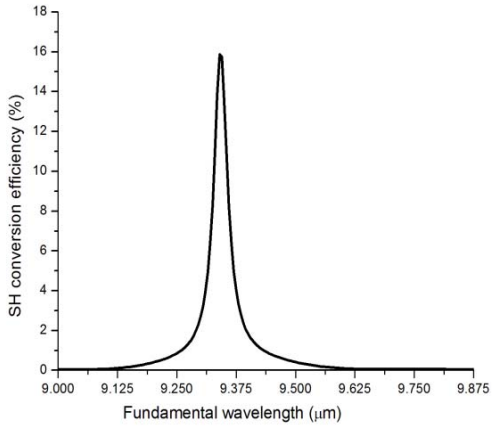

Fig. 2. Plot of SH efficiency vs input wavelength for CdTe slab for ψ = 0.394 rad, ϕ_i= 1.4 rad, L =10 mm, t= 400 μm, considering all the losses (scattering, absorption, GH shift) encountered by the interacting waves.

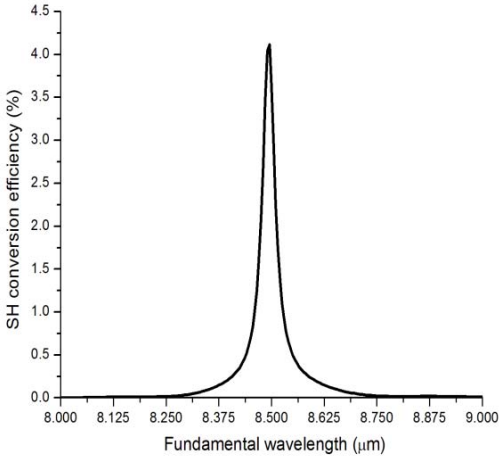

Fig. 3. Plot of SH efficiency vs input wavelength for ZnTe slab for ψ = 0.394 rad, ϕ_i= 1.4 rad, L =10 mm, t= 400 μm, considering all the losses (scattering, absorption, GH shift) encountered by the interacting waves.

With variation in the angle of incidence, ϕ_i, both ZnTe and CdTe show a shift in the center wavelength corresponding to peak efficiency. For ZnTe as ϕ_i is decreased from 1.4 rad to 1.1 rad, the center wavelength shows a red shift in its value from 8.508 μm to 8.58 μm while the peak efficiency increases from 4.13% to 4.918%. With CdTe, for similar variation in ϕ_i, the center wavelength shows a red shift from 9.342 μm to 9.434 μm while the efficiency increases from 15.89% to 18.67%. Fig. 4 and Fig. 5 show the performance of both the materials due to variation in ϕ_i.

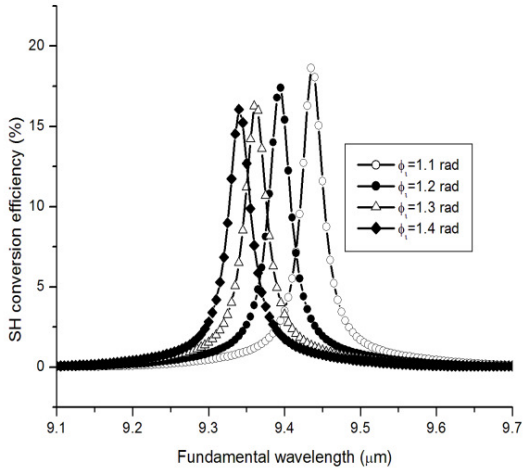

Fig. 3. Plot of SH efficiency vs input wavelength for CdTe slab for varying values of ϕ_i.

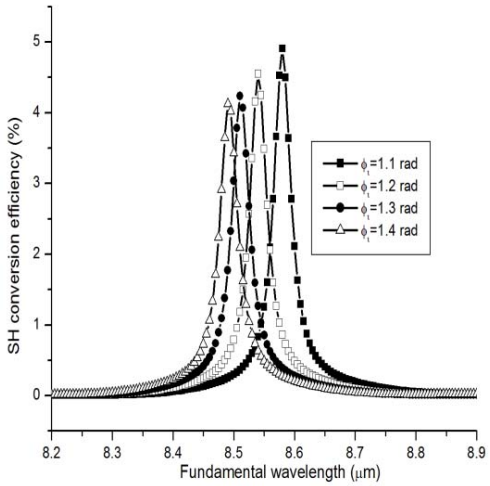

Fig. 4. Plot of SH efficiency vs input wavelength for ZnTe slab for varying values of ϕ_i.

IV. CONCLUSION

To conclude in this paper, a SH frequency converter based on a parallel ZnTe and CdTe slab has been analysed numerically. The converter provides conversion efficiencies of 4.13% (centered at 8.508 μm) and 15.89% (centered at 9.34 μm) in a 400 μm thick, 10-mm-long slab of ZnTe and CdTe respectively, considering losses due to surface roughness, Goos-Hänchen shift and material absorption. Variation in the angle of incidence results in red shift of the center wavelength of both the materials under study and hence can be used for angle tuning of the center wavelength corresponding to peak efficiency.

REFERENCES

[1] D. Richter, A. Fried, and E. K. Tittel, "Trends in Laser Sources, Spectroscopic Techniques and Their Applications to Trace Gas Detection," Appl. Phys. B., vol. 75, pp. 391-396, 2002.

[2] E. Rosencher, Onwards all-semiconductor integrated optical parametric oscillator. C. R. Acad. Sci. Paris, Serie IV . 2000, pp. 615-625.

[3] http://en.wikipedia.org/wiki/ZnTe

[4] J. A. Armstrong, N. Bloembergen, J. Ducuing, and P. S. Pershan, "Interactions between light waves in a nonlinear dielectric," Phys. Rev., vol. 127, pp. 1918-1939, 1962.

[5] G. D. Boyd and C. K. N. Patel, "Enhancement of optical second harmonic generation (SHG) by reflection phase- matching in ZnS and GaAs," Appl. Phys. Lett., vol. 8, pp. 313-315, 1966.

[6] H. Komine, W. H. Long, Jr., J. W. Tully, and E. A. Stappaerts, "Quasi-phase-matched second-harmonic generation by use of a total-internal-reflection phase shift in gallium arsenide and zinc selenide plates," Opt. Lett., vol. 23, pp. 661-663, 1998.

[7] R. Haïdar, N. Forget, P. Kupecek, and E. Rosencher, "Fresnel phase matching for three-wave mixing in isotropic semiconductors," J. Opt. Soc. Am. B., vol. 21, pp. 1522-1534, 2004.

[8] http://www.clevelandcrystals.com/II-VI.htm

[9] D. T. F. Marple, "Refractive index of ZnSe, ZnTe, and CdTe," J. Appl. Phys., vol. 35, pp. 539-542, 1964.

[10] A. W. Snyder and J. D. Love, "Goos-Hänchen shift," Appl. Opt., vol. 15, pp. 236-238, 1976.